

User Association Schemes for Cellular Networks

A Project Report

submitted by

ATHINDRAN RAMESH KUMAR

(EE09B100)

in partial fulfilment of the requirements

for the award of the degree of

BACHELOR OF TECHNOLOGY

in

ELECTRICAL ENGINEERING



**DEPARTMENT OF ELECTRICAL ENGINEERING
INDIAN INSTITUTE OF TECHNOLOGY, MADRAS.**

MAY 2013

PROJECT CERTIFICATE

This is to certify that the project titled **User Association Schemes for Cellular Networks**, submitted by **R. Athindran (EE09B100)**, to the Indian Institute of Technology, Madras, for the award of the degree of **Bachelor of Technology**, is a bonafide record of the project work done by him under my supervision. The contents of this report, in full or in parts, have not been submitted to any other Institute or University for the award of any degree or diploma.

Prof. Radhakrishna Ganti

Project Guide

Professor

Dept. of Electrical Engineering

IIT Madras, Chennai 600 036

Prof. Enakshi Bhattacharya

Head

Dept. of Electrical Engineering

IIT Madras, Chennai 600 036

Place: Chennai

Date: May 17, 2013

ACKNOWLEDGEMENTS

Firstly, I would like to thank Prof. Radhakrishna Ganti for the continued support and motivation over the past one year. His moral support and guidance right from the conception to the completion of the project has helped me to a large extent. I would also like to thank my professors and friends through the course of my undergraduate study. The experience of interacting with such elite people has truly transformed me. Special thanks to Rohan Sriram, Ravi Kiran, Sai Venkatesh and Archith for their ideas during the course of my project. Last but not the least, I would like to thank my parents for their unwavering support throughout the course of my degree. I would not be what I am today if not for their sacrifices.

ABSTRACT

KEYWORDS: Poisson Point Process ; Cellular network; Coverage probability; User rate ; Cell association scheme.

Cellular networks are undergoing a paradigm shift with the number of base stations (BSs) increasing rapidly every year. This calls for a change in the techniques used for modeling, analyzing, simulating and designing cellular networks.

The hexagonal grid model in which the BSs are placed in a lattice is not very tractable and does not capture the opportunistic and dense placement of base stations in futuristic networks. Further the rate distribution of users is a better performance metric than the outage probability for rating the quality of service in such networks. This work models the BSs as randomly and uniformly distributed in space. In the absence of prior information, this is regarded as the best statistical model. Further, alternative cell association schemes which optimize the rate distribution rather than SINR are discussed. These association schemes, which focus on load balancing , are effective in improving the quality of service, especially in networks with heterogeneity.

TABLE OF CONTENTS

ACKNOWLEDGEMENTS	i
ABSTRACT	ii
LIST OF FIGURES	1
1 Introduction	2
1.1 Downlink system model	2
1.2 Need for alternative cell association schemes	4
1.3 Organization of the thesis	6
2 Point Process Theory- A review	7
2.1 Stationary Poisson Point Process	8
2.1.1 Distance properties of a PPP	8
2.1.2 Sums and Products over a stationary PPP	10
2.1.3 Transformations of PPP (Independent thinning) . .	10
2.1.4 Conditioning and Palm Probability	11
3 Alternative Association Scheme for Cell Users	12
3.1 Assumptions	12
3.2 Coverage	13
3.3 Rate	19
4 Complex Association Schemes	24

4.1	Bandwidth maximization by choosing between multiple base stations	24
4.2	SINR biasing	26
4.2.1	Single-Tier Network	27
4.2.2	Three-tier heterogeneous network	28
5	Conclusions and future work	30

LIST OF FIGURES

3.1	The above plot shows the variation of coverage probability with threshold θ for two cases. In case 1 ($p = 0$), the user connects with the nearest base station while in case 2 ($p = 1$), the user connects with the second nearest base station. .	19
3.2	Density of base stations $\lambda_b = 0.03$, Density of users $\lambda_u = 0.9$, Loss function $l(x) = \frac{1}{1+\ x\ ^\alpha}$, Path loss exponent $\alpha = 4$ and Noise variance $\sigma^2 = 1$	21
3.3	Density of base stations $\lambda_b = 0.03$, Density of users $\lambda_u = 0.9$, Loss function $l(x) = \ x\ ^{-\alpha}$, Path loss exponent $\alpha = 4$ and Noise variance $\sigma^2 = 1$	22
3.4	The above plot shows the variance in the number of users in a cell for $\lambda_b = 0.03, \lambda_u = 0.9$	23
4.1	The above plot shows the variation of average rate with increasing base station density. The density of users $\lambda_u = 0.8$. It is seen that the rate increases with base station density and converges to a value in both the association schemes. .	25
4.2	The above plot shows the variation of average SINR with increasing base station density. The density of users $\lambda_u = 0.8$. It is seen that the SINR of a typical user sharply decreases and remains constant for high base station densities. Further, it is seen that the nearest BS scheme gives a higher SINR.	25
4.3	The above plot shows the variation of the average number of users of an associating base station with increasing base station density. The density of users $\lambda_u = 0.8$. It is seen that the average number of users of an associating base station is lesser for the bandwidth maximizing scheme.	26

4.4	The SINR bias scheme is compared with the max-SINR and the nearest BS scheme for a single-tier network. Upon introducing a bias, the average rate of the SINR bias scheme is seen to be lesser than the max-SINR scheme. The increased bandwidth due to load balancing is not enough to improve the rate due to association with BSs providing sub-optimal SINRs.	27
4.5	The above plot compares the max-SINR scheme with the SINR biasing scheme for a 3-tier cellular network, in terms of mean rate. Bias weights of 1 and 3 are assigned to the first and second tiers. The average rate is then seen to increase with the bias weight of the third tier from the above plot. .	28
4.6	For the 3-tier cellular network described in 4.2.2, bias weights of 1, 3 and 20 are assigned to the 1st, 2nd and 3rd tiers respectively. The rate CDF of the SINR biasing scheme is then obtained as above. Note that the rates of edge users are particularly boosted by the SINR bias scheme.	29

CHAPTER 1

Introduction

Due to the heavy proliferation of smart phones, laptops , tablets with cellular connections, there is an ever increasing demand for capacity. The only scalable way to meet this demand is by increasing the number of base stations. As a result, grid models which place base stations in a lattice are highly idealized and do not capture the dense and opportunistic placement of base stations in futuristic networks. Further, the techniques used for modeling, analyzing and simulating cellular networks also need re-evaluation. In (2), seven important changes in the way cellular networks need to be studied are discussed. (2) calls for the use of Poisson models, in which the base stations are randomly distributed in space. Further, the need for alternative cell association schemes, which focus on improving the rate distribution rather than the SINR, is emphasized.

1.1 Downlink system model

Traditional approaches to model base stations in a cellular network include the Wyner model and the hexagonal grid based model. The Wyner model assumes a unit gain from each base station to the tagged user and an equal gain that is less than one to all users in the neighbouring cells. Such a model does not differentiate between interior and edge users and hence there is no notion of outage. This model is tractable but highly inaccurate

due to the simplifying assumptions. Another popular model is to place the base stations in a hexagonal grid. In (3) and (4), a hexagonal grid model is used for the base stations, and the SINR analysis is performed assuming worst-case user location - the cell corner. However, tractable expressions for SINR and coverage probability for a user at a random position in the cell, can only be arrived at by complex time-consuming simulations. Further the grid models are very idealized as cell radii may vary considerably in future networks, due to differences in transmission power, tower height and user density.

Based on the recommendation in (2), a Poisson BS model, in which the BS's are placed randomly, is used in this work. In this model of a cellular network, the base stations are distributed according to a homogeneous Poisson point process (PPP) Φ_b of density λ_b in the Euclidean plane. Further, the users are also assumed to be distributed according to another homogeneous PPP of density λ_u . Such an approach for base station modeling was considered in (8; 9), but the metrics of coverage and rate were not determined. In (1), the expressions for coverage and rate for a typical user in a single-tier cellular network have been obtained using tools from stochastic geometry. Despite the controversial independence assumption, this model is found to more tractable and as accurate as the previously used hexagonal grid model. However, this Poisson model also suffers from a few drawbacks. The main weakness of the Poisson model is that because of the independence of the PPP, BSs will in some cases be located very close together but with a significant coverage area. This weakness is balanced by two strengths: the natural inclusion of different cell sizes and shapes and the lack of edge effects, i.e. the network extends indefinitely in all directions.

In this work, two power loss propagation models have been used with power loss exponent $\alpha = 4$. These are

$$l_1(x) = \|x\|^{-\alpha},$$

$$l_2(x) = \frac{1}{1 + \|x\|^\alpha}.$$

The power loss model used has been explicitly mentioned before each analysis or simulation. As far as random channel effects such as fading and shadowing, we assume that the tagged base station and tagged user experience only Rayleigh fading with mean 1.

1.2 Need for alternative cell association schemes

The two metrics commonly used to rate the performance of cellular networks are the coverage probability (CCDF of SINR) and the spectral efficiency. With the increase in the number of base stations, the base station placement and their distribution have become increasingly random. As a result, there will be some base stations which are lightly loaded as compared to others. In such a scenario, the application level data rate depends not only on the SINR but also the load. A better performance metric for such networks would be the rate distribution and not the coverage probability.

Thus, the traditional scheme of associating users with the nearest base station (or maximum SINR) may no longer be optimal. When the users are

associated with base stations using the maximum-SINR scheme, there will be unequal loads on different base stations due to disparities in cell sizes. The users which are associated with a heavily congested base station will be severely affected. Pushing users from heavily loaded base stations to lightly loaded base stations can be beneficial. Hence, we seek alternative cell association schemes where the load is more evenly balanced among the base stations.

(7) classifies the previous work on cell association into two categories:

1. Strategies based on channel borrowing from lightly-loaded cells, such as Hybrid Channel Assignment (HCA), and load balancing with selective borrowing.
2. Strategies based on traffic transfer to lightly loaded cells such as Directed Retry, hierarchical macro-cell overlay systems, cell breathing techniques and biasing methods.

This work focuses mainly on traffic transfer strategies which shift users from heavily loaded cells to lightly loaded cells. Some of the existing traffic transfer strategies are dynamic schemes. For instance, the cell breathing technique (12) dynamically changes the coverage area depending on the load situation by controlling the transmit power. In (11), biasing techniques for cell-range expansion in heterogeneous networks are discussed. In this work, a simple association scheme where the users connect with either the first nearest or the second nearest base station is studied. This scheme is found to be considerably effective in balancing the load among the base stations. Further, the SINR biasing scheme is studied for a single-tier cellular network and a 3-tier cellular network and the difference in performance is noted.

1.3 Organization of the thesis

The thesis is organized as follows. In chapter 2, some results from point process theory and stochastic geometry which are used for obtaining expressions for coverage probability and rate, are reviewed. In chapter 3, an alternative association scheme where a user connects either with the first nearest or the second nearest base stations with fixed probabilities is introduced. Using the results from stochastic geometry, an expression for coverage probability is derived for a cellular network which uses this alternative association scheme. The mean rate and rate variance are obtained through MATLAB simulations. In chapter 4, an allocation scheme in which the user connects to a base station with least load is studied. Further, the performance of the SINR bias scheme in a single tier and a 3-tier network is compared.

CHAPTER 2

Point Process Theory- A review

In this chapter, we review some of the basic definitions and results from Point Process theory which play a major role in our analysis of cellular networks.

Definition: The mathematical definition of a point process on \mathbb{R}^2 is as a random variable taking values in a measurable space \mathbb{N} , where \mathbb{N} is the family of all sequences φ of points of \mathbb{R}^2 satisfying two regularity conditions:

1. that the sequence φ is locally finite (each bounded subset of \mathbb{R}^2 must contain only a finite number of points of φ),
2. that the sequence is simple (so $x_i \neq x_j$ if $i \neq j$).

Point processes can be considered either as random sets of discrete points or as random measures counting the number of points lying in spatial regions. Corresponding to this are two different notations:

- A point process is denoted by Φ ; An instance of the point process is denoted by ϕ . $x \in \Phi$ asserts that x belongs to the random sequence ϕ .
- $\Phi(B) = n$ asserts that the set B contains n points of Φ .

Some characteristics of a point process include:

- A simple point process Φ is determined by its void probabilities over all compact sets, i.e. , $\mathbb{P}(\Phi(K) = 0)$ for $K \subset \mathbb{R}^2$ and compact.
- Stationarity : A Poisson point process is said to be stationary if its distribution is invariant to translations.

2.1 Stationary Poisson Point Process

In this work, we use a stationary Poisson point process to model the base station distribution. A stationary Poisson point process Φ of density λ is characterized by

1. The number of points in a bounded Borel set $B \subset \mathbb{R}^2$ has a Poisson distribution with mean $\lambda |B|$

$$\mathbb{P}(\Phi(B) = m) = \frac{(\lambda |B|)^m}{m!} \cdot \exp(-\lambda |B|)$$

for $m = 0, 1, 2 \dots$

2. The number of points in k disjoint Borel sets form k independent random variables.

We now present some of the interesting properties and results of the stationary PPP. For proofs of the following results and a more detailed understanding of the PPP, please refer (5), (6).

Lemma 2.1.1 *Let $A \subset \mathbb{R}^2$. Conditioned on the number of points in $\Phi(A)$, the points are independently and uniformly distributed in the set A .*

Thus, the simulation of a stationary PPP in a compact region W can be divided into two stages. First, the number of points in W is determined by simulating a Poisson random variable. From lemma 2.1.1, we know that these points can be uniformly distributed in the region W .

2.1.1 Distance properties of a PPP

Lemma 2.1.2 *First contact distribution - The CCDF of the distance of the nearest point of the process from the origin o denoted by r is $\mathbb{P}(r \geq r_1) = \exp(-\lambda \pi r_1^2)$*

and the PDF of r is given by $f_1(r) = 2\lambda\pi r \exp(-\lambda\pi r^2)$.

Proof : From the definition of a PPP, we obtain,

$$\mathbb{P}[r > r_1] = \mathbb{P}(B(o, r_1) \text{ is empty}) = \exp(-\lambda\pi r_1^2).$$

The CDF is thus given by $F_{r_1}(R) = 1 - \exp(-\lambda\pi R^2)$ Therefore, the pdf is given by :

$$\begin{aligned} f_1(r_1) &= \frac{d}{dr_1}(F_{r_1}(r_1)) \\ &= 2\lambda\pi r_1 \exp(-\lambda\pi r_1^2). \end{aligned}$$

Lemma 2.1.3 *Joint distribution - The joint pdf of the distances of the two nearest points to the origin o , denoted by r_1 and r_2 , is given by $f_{12}(r_1, r_2) = 4\lambda^2\pi^2 r_1 r_2 \exp(-\lambda\pi r_2^2)$.*

The joint distribution $f_{12}(r_1, r_2)$ can also be derived using similar techniques. We note that :

$$\begin{aligned} \mathbb{P}(r_1 < R_1, r_2 < R_2) &= 1 - \mathbb{P}(\Phi_b(B(o, R_1)) = 0) - \\ &\quad \mathbb{P}(\Phi_b(B(o, R_1)) = 1) \mathbb{P}(\Phi_b(B(o, R_2) - B(o, R_1)) = 0) \end{aligned}$$

$$\mathbb{P}(r_1 < R_1, r_2 < R_2) = 1 - \exp(-\lambda\pi r_1^2) - \lambda\pi r_1^2 \exp(-\lambda\pi r_2^2)$$

The joint CDF is thus given by $F_{12}(r_1, r_2) = 1 - \exp(-\lambda\pi r_1^2) - \lambda\pi r_1^2 \exp(-\lambda\pi r_2^2)$.
Thus,

$$\begin{aligned}
f_{12}(r_1, r_2) &= \frac{d}{dr_1} \left(\frac{d}{dr_2} (F_{12}(r_1, r_2)) \right) \\
&= 4\lambda^2 \pi^2 r_1 r_2 \exp(-\lambda \pi r_2^2).
\end{aligned}$$

2.1.2 Sums and Products over a stationary PPP

Lemma 2.1.4 (*Campbell's theorem*) Let Φ be a PPP of density λ and $f(x) : \mathbb{R}^2 \rightarrow \mathbb{R}^+$.

$$\mathbb{E}_{x \in \Phi} [f(x)] = \lambda \int_{\mathbb{R}^2} f(x) dx.$$

Refer (5) for proof.

Lemma 2.1.5 (*Probability generating functional*) Let Φ be a PPP of density λ and $f(x) : \mathbb{R}^2 \rightarrow [0, 1]$ be a real valued function. Then

$$\mathbb{E} \left[\prod_{x \in \Phi} f(x) \right] = \exp \left(-\lambda \int_{\mathbb{R}^2} (1 - f(x)) dx \right).$$

Refer (5) for proof.

2.1.3 Transformations of PPP (Independent thinning)

Let Φ be a stationary PPP of density λ .

1. A node $x \in \Phi$ is of type 1 with probability p and of type 2 with probability $1 - p$.
2. Let Φ_1 denote the type 1 point process and Φ_2 denote the type 2 point process. Thus we have $\Phi = \Phi_1 + \Phi_2$.

Lemma 2.1.6 Φ_1 and Φ_2 are independent PPPs with densities λp and $\lambda(1 - p)$.

Proof : Look at the void probabilities of Φ_1 and Φ_2 .

2.1.4 Conditioning and Palm Probability

Many problems in point process theory require the consideration of an arbitrary “typical” point of a point process Φ . In intuitive terms, the palm distribution probabilities are the conditional probabilities of point process given that a point is observed at a specific location. If Y is some point process property, then we set

$$\mathbb{P}(\Phi \text{ has property } Y \| x) = \mathbb{P}(\Phi \text{ has property } Y \mid x \in \Phi).$$

The reduced palm distribution $P_x^!$ is defined

$$P_o^!(Y) = P(\Phi \setminus \{o\} \text{ has property } Y \| o).$$

Intuitively, the reduced palm distribution can be interpreted as probability conditioned on there being a point at the origin, but not counting it.

Theorem 2.1.1 *Slivnyak Theorem* - The reduced palm distribution of a PPP equals the original distribution, i.e $P_o^! = P$.

CHAPTER 3

Alternative Association Scheme for Cell Users

Usually, each user in a cellular network is linked with the nearest base station to maximize the SINR of the user. However, the load distribution might be highly non-uniform in this scenario. Here, another association scheme is studied in terms of the probability of coverage, average SINR and rate. In this scheme, the user is linked with the nearest base station with probability $1 - p$ and with the second nearest base station with probability p . The base stations and users of a cellular network are modeled as two independent homogeneous Poisson point processes of intensities λ_b and λ_u respectively. Some assumptions used in the analysis are listed below.

3.1 Assumptions

1. Fading between any two nodes is Rayleigh , i.e the fading power is exponentially distributed with unit mean.

$$P(h_{xy} \geq z) = \exp(-z) \quad (3.1)$$

2. The path loss function $l(x)$ is given by,

$$l(x) = \|x\|^{-\alpha}$$

,where $\|x\|$ is the distance of the point from the source.

3. The interference power at the typical receiver I_r is the sum of the received powers from all other base stations other than the home

base station and is treated as noise in the present work. The receiver noise is neglected in comparison with interference.

4. All analysis is for a typical mobile node which is permissible in a homogeneous PPP by Slivnyak's theorem

3.2 Coverage

In this section, we derive the probability of coverage in a downlink cellular network, with the alternative allocation scheme that is being proposed. The coverage probability can be thought of as the probability that a user chosen at random can achieve a target SINR θ . Mathematically, the coverage probability is defined as

$$p_c(\theta, \lambda_b, \alpha) = \mathbb{P}(SINR > \theta).$$

Note that the probability of coverage is also exactly the CCDF of SINR over the entire network, since the CDF gives $\mathbb{P}(SINR < \theta)$. To perform the analysis, we assume the typical mobile user at the origin o . The downlink SIR at the origin is given by :

$$SIR = \frac{h_{xo}l(x)}{\sum_{y \in \Phi_b \setminus \{x\}} h_{yo}l(y)}$$

, when x is the nearest base station.

Nearest base station distributions

For our analysis, we are concerned with the distances r_1 and r_2 separating a typical user from the first and second nearest base stations respectively. From Slivnyak's theorem (Theorem 2.1.1), we know that the contact distributions equal the distribution of the nearest neighbour distances. Therefore, the pdf is given by :

$$f_1(r_1) = 2\lambda\pi r_1 \exp(-\lambda\pi r_1^2).$$

The joint distribution $f_{12}(r_1, r_2)$ is thus given by,

$$f_{12}(r_1, r_2) = 4\lambda^2\pi^2 r_1 r_2 \exp(-\lambda\pi r_2^2).$$

Analysis

We now use the nearest base station distributions to find the expected coverage. A typical user at the origin can connect with the nearest base station B_1 with probability $1 - p$ and the second nearest base station B_2 with probability p . Let x denote the connecting base station.

$$\begin{aligned} \mathbb{P}(SIR > \theta) &= \mathbb{P}\left(\frac{h_{xo}l(x)}{\sum_{y \in \Phi_b \setminus \{x\}} h_{yo}l(y)} > \theta\right) \\ &= (1 - p) \times \mathbb{P}\left(\frac{h_{xo}l(x)}{\sum_{y \in \Phi_b \setminus \{x\}} h_{yo}l(y)} > \theta \middle| x \equiv B_1\right) \\ &\quad + (p) \times \mathbb{P}\left(\frac{h_{xo}l(x)}{\sum_{y \in \Phi_b \setminus \{x\}} h_{yo}l(y)} > \theta \middle| x \equiv B_2\right) \end{aligned}$$

Let $P_1 = \mathbb{P} \left(SINR > \theta \middle| x \equiv B_1 \right)$ and $P_2 = \mathbb{P} \left(SINR > \theta \middle| x \equiv B_2 \right)$

Now, we go ahead and obtain expressions for P_1 and P_2 separately. In (1), the expression for P_1 is derived. The analysis is shown below.

$$\begin{aligned} P_1 &= \mathbb{P}(SIR > \theta \middle| x \equiv B_1) \\ &= \mathbb{E}_{r_1} \left(\mathbb{P} \left(SIR > \theta \middle| x \equiv B_1, \|B_1\| = r_1 \right) \right) \end{aligned}$$

Again,

$$\begin{aligned} p_{r_1} &= \mathbb{P} \left(SIR > \theta \middle| x \equiv B_1, \|B_1\| = r_1 \right) = \mathbb{P} \left(\frac{h_{xo}l(x)}{\sum_{y \in \Phi_b \setminus \{x\}} h_{yo}l(y)} > \theta \middle| x \equiv B_1, \|B_1\| = r_1 \right) \\ &= \mathbb{P} \left(\frac{h_{xo}r_1^{-\alpha}}{I_r} > \theta \middle| x \equiv B_1, \|B_1\| = r_1 \right) \\ &= \mathbb{E}_{I_r} \left(\mathbb{P} \left(h_{xo} > \theta I_r r_1^\alpha \middle| x \equiv B_1, \|B_1\| = r_1, I_r \right) \right) \\ &= \mathbb{E}_{I_r} \left(\exp(-\theta r^\alpha I_r) \middle| r_1 \right) \\ &= \mathbb{E} \left(\exp \left(-\theta r^\alpha \sum_{y \in \Phi_b \setminus \{x\}} h_{yo}l(y) \right) \middle| r_1 \right). \end{aligned}$$

By substituting the path loss function $l(y) = \|y\|^{-\alpha}$, we get

$$\begin{aligned} p_{r_1} &= \mathbb{E} \left(\exp \left(-\theta r^\alpha \sum_{y \in \Phi_b \setminus \{x\}} h_{yo} \|y\|^{-\alpha} \right) \middle| r_1 \right) \\ &= \mathbb{E} \left(\prod_{y \in \Phi_b \setminus \{x\}} \exp \left(-\theta r^\alpha h_{yo} \|y\|^{-\alpha} \right) \middle| r_1 \right). \end{aligned}$$

Since the fades are independent and exponentially distributed with unit mean,

$$p_{r_1} = \mathbb{E} \left(\prod_{y \in \Phi_b \setminus \{x\}} \frac{1}{1 + \theta r_1^\alpha \|y\|^{-\alpha}} \middle| r_1 \right). \quad (3.2)$$

Using PGFL (Refer Lemma 2.1.5) on $\Phi \cap B(o, r_1)^c$,

$$p_{r_1} = \exp \left(-\lambda \int_{B(o, r)^c} \frac{1}{1 + \theta^{-1} r_1^{-\alpha} \|y\|^\alpha} dy \right).$$

Thus,

$$P_1 = E_{r_1} (p_{r_1}) = \int_{r_1=0}^{\infty} \exp \left(-\lambda \int_{B(o, r)^c} \frac{1}{1 + \theta^{-1} r_1^{-\alpha} \|y\|^\alpha} dy \right) f_1(r_1) dr_1,$$

where

$$f_1(r_1) = \lambda 2\pi r_1 \exp \left(-\lambda \pi r_1^2 \right).$$

From (1), we know that

$$P_1 = \frac{1}{1 + F(\theta, \alpha)}, \quad (3.3)$$

where $F(\theta, \alpha) = \theta^{\frac{2}{\alpha}} \int_{\theta^{\frac{-2}{\alpha}}}^{\infty} \frac{1}{1 + u^{\frac{\alpha}{2}}} du$.

Using a similar procedure, we set about obtaining an expression for P_2 ,

$$\begin{aligned} P_2 &= \mathbb{P} \left(\frac{h_{xo}l(x)}{\sum_{y \in \Phi_b \setminus \{x\}} h_{yo}l(y)} > \theta \middle| x \equiv B_2 \right) \\ &= \mathbb{E}_{r_1, r_2} \left(\mathbb{P} \left(\frac{h_{xo}l(x)}{\sum_{y \in \Phi_b \setminus \{x\}} h_{yo}l(y)} > \theta \middle| x \equiv B_2, \|x\| = r_2, \|B_1\| = r_1 \right) \right). \end{aligned}$$

Again, let

$$p_{r_1, r_2} = \mathbb{P} \left(\frac{h_{xo}l(x)}{\sum_{y \in \Phi_b \setminus \{x\}} h_{yo}l(y)} > \theta \middle| x \equiv B_2, \|x\| = r_2, \|B_1\| = r_1 \right).$$

The fades h_{xo} for $x \in \Phi_b$ are independent and exponentially distributed with unit mean. Repeating steps used for deriving equation 3.2, we find the expectation over the fades h_{xo} for $x \in \Phi_b$ and get

$$\begin{aligned} p_{r_1, r_2} &= \mathbb{E}_{\Phi \setminus B_1, x} \left[\prod_{y \in \Phi_b \setminus x} \frac{1}{1 + \theta r_2^\alpha \|y\|^{-\alpha}} \right] \\ &= \mathbb{E}_{\Phi \setminus x, B_1} \left[\prod_{y \in \Phi_b \setminus x, B_1} \frac{1}{1 + \theta r_2^\alpha \|y\|^{-\alpha}} \right] \cdot \left(\frac{1}{1 + \theta r_2^\alpha r_1^{-\alpha}} \right). \end{aligned}$$

Using PGFL on $\Phi \cap B(o, r_2)^c$, we get

$$p_{r_1, r_2} = \frac{\exp(-\lambda \pi r_2^2 F(\theta, \alpha))}{1 + r_2^\alpha r_1^{-\alpha}}$$

where $F(\theta, \alpha) = \theta^{\frac{2}{\alpha}} \int_{\theta^{\frac{2}{\alpha}}}^{\infty} \frac{1}{1 + u^{\frac{\alpha}{2}}} du$.

Thus

$$P_2 = \int_0^\infty \int_0^{r_2} \frac{\exp(-\lambda\pi r_2^2 F(\theta, \alpha))}{1 + r_2^\alpha r_1^{-\alpha}} f_{12}(r_1, r_2) dr_1 dr_2$$

, where $f_{12}(r_1, r_2) = 4\lambda^2\pi^2 r_1 r_2 \exp(-\lambda\pi r_2^2)$.

Making the substitution $\beta = r_2$ and $t = \frac{r_2}{r_1}$, we get

$$\begin{aligned} P_2 &= \left(4\lambda^2\pi^2 \int_{\beta=0}^\infty \beta^3 \exp(-\lambda\pi\beta^2(1 + F(\theta, \alpha))) d\beta \right) \times \int_{t=1}^\infty \frac{dt}{t^3(1 + t^\alpha)} \\ &= \frac{2}{(1 + F(\theta, \alpha))^2} \times \int_{t=1}^\infty \frac{dt}{t^3(1 + \theta t^\alpha)}. \end{aligned}$$

Therefore,

$$\mathbb{P}(SINR > \theta) = (1 - p) \times \frac{1}{1 + F(\theta, \alpha)} + p \times \frac{2q}{(1 + F(\theta, \alpha))^2}, \quad (3.4)$$

$$\text{where } q = \int_{t=1}^\infty \frac{dt}{t^3(1 + t^\alpha)}.$$

The expression for coverage probability is substituted from equation 3.4 and the integral is computed numerically. Figure 3.1 is obtained from the computations.

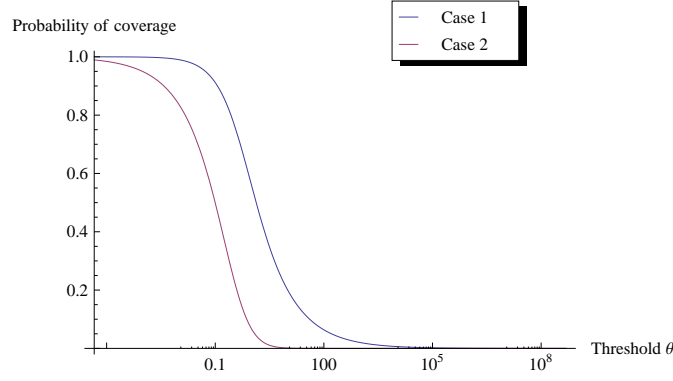


Figure 3.1: The above plot shows the variation of coverage probability with threshold θ for two cases. In case 1 ($p = 0$), the user connects with the nearest base station while in case 2 ($p = 1$), the user connects with the second nearest base station.

3.3 Rate

The normalized rate of a user after load allocation is given by

$$r = \frac{W}{N} \log(1 + SINR),$$

where W is the bandwidth available to the connecting base station and N is the number of coexisting users connected to the same base station.

Thus,

$$\mathbb{E}[r] = W \cdot \mathbb{E} \left[\frac{1}{N} \log(1 + SINR) \right].$$

The analysis behind obtaining an expression for N is not well under-

stood. This makes the analysis of the expected rate and rate variance rather difficult. Further, one can also introduce the concept of a minimum rate threshold for every user in a cellular network. Whenever the SINR does not meet this requirement, the user is said to go out of coverage and a rate of 0 is assigned. Please note that this notion of coverage is different from the one studied in the previous section. Here we have a minimum rate threshold and not SINR threshold to ensure coverage.

$$\text{Condition for coverage : } \frac{W}{N} \log_2(1 + \text{SINR}) > R_{th} \text{ or } \text{SINR} > 2^{\frac{R_{th}N}{W}} - 1.$$

Simulation studies of our model can help get better insights of the alternative association scheme in terms of the mean rate achievable, especially in the presence of receiver noise and rate thresholds. Thus, the homogeneous PPP's for the base stations and the users in a cellular network are simulated in MATLAB. The users are assigned base stations according to the alternative assignment scheme that was analyzed in the previous section. Based on the simulation results, the average rate, variance in rate among users, average SINR and the coverage are plotted as a function of the parameter p .

The figures 3.2, 3.3 and 3.4 show the results of the simulation for varying base station densities and different choices of the path loss function. While the average rate decreases with p in general, it is found that the variance in rate also decreases as p increases.

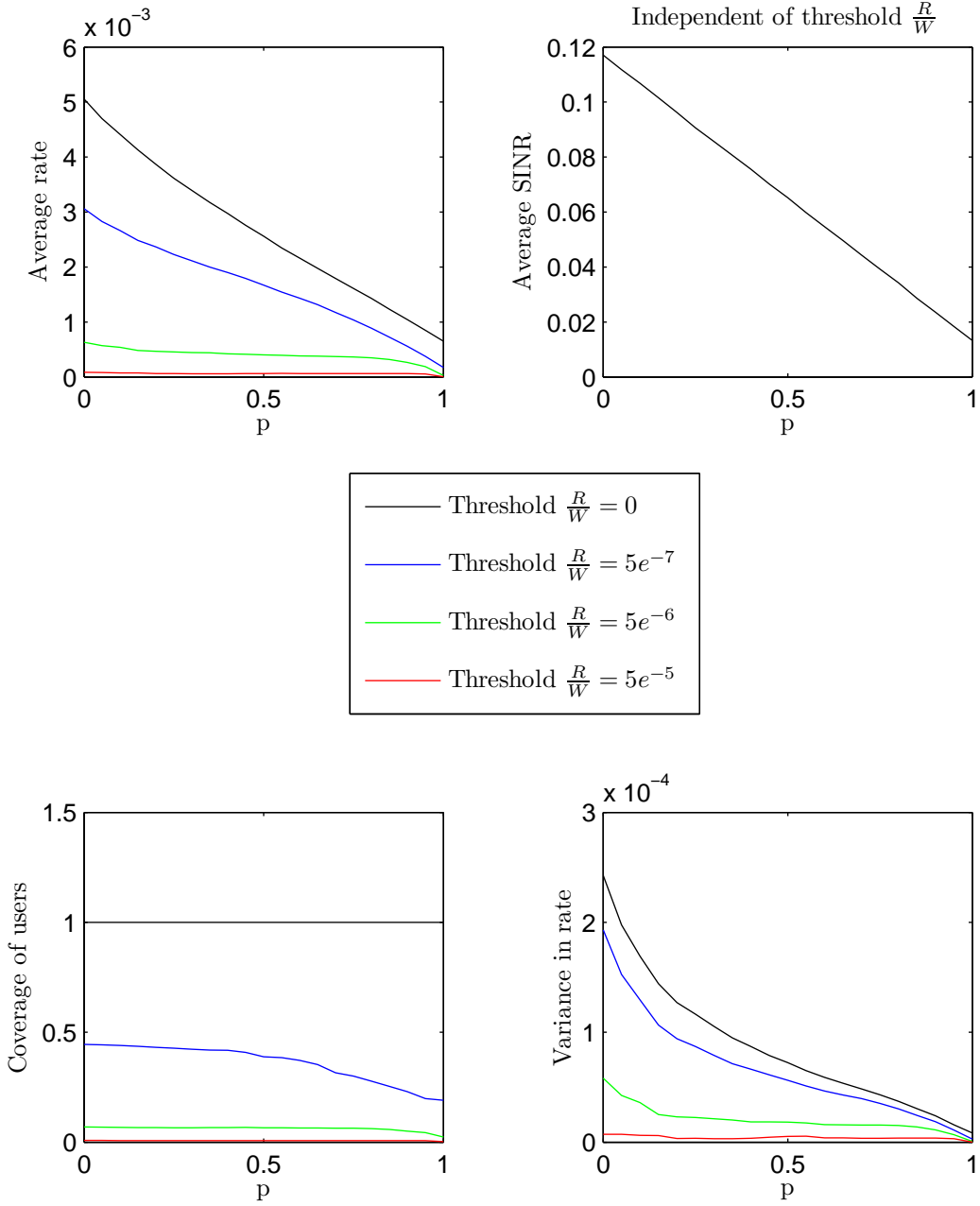


Figure 3.2: Density of base stations $\lambda_b = 0.03$, Density of users $\lambda_u = 0.9$,
Loss function $l(x) = \frac{1}{1+\|x\|^\alpha}$, Path loss exponent $\alpha = 4$ and
Noise variance $\sigma^2 = 1$.

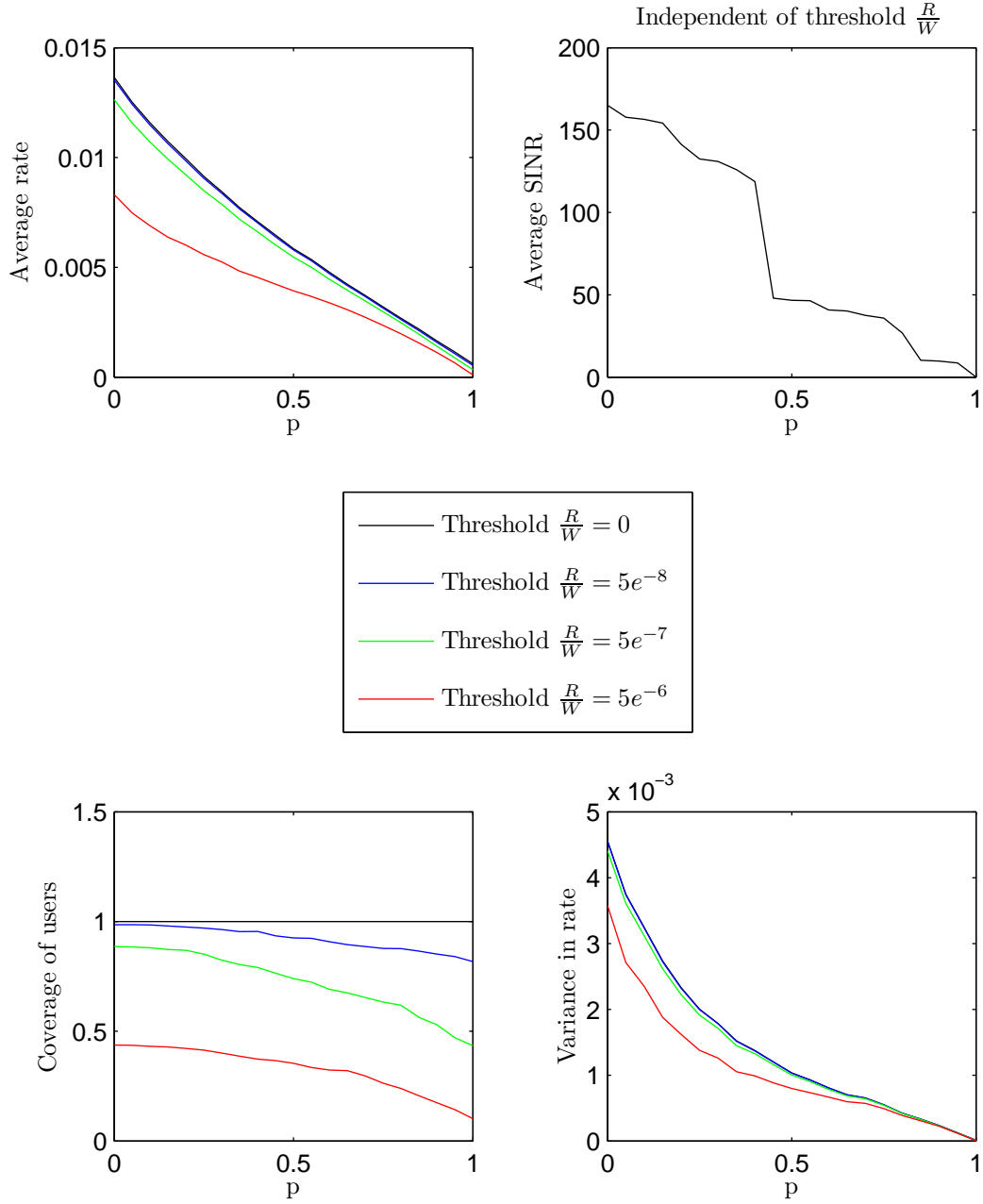


Figure 3.3: Density of base stations $\lambda_b = 0.03$, Density of users $\lambda_u = 0.9$, Loss function $l(x) = \|x\|^{-\alpha}$, Path loss exponent $\alpha = 4$ and Noise variance $\sigma^2 = 1$.

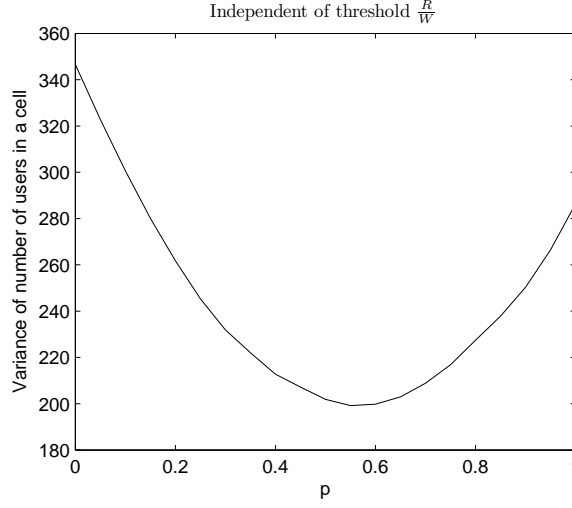


Figure 3.4: The above plot shows the variance in the number of users in a cell for $\lambda_b = 0.03, \lambda_u = 0.9$.

From figure 3.4, we note that variance in number of users per base station is minimum for p between 0.5 and 0.6. This implies that the load is more evenly balanced among the base stations. However from figures 3.2 and 3.3, we note that the rate also falls considerably due to the fall in SINR. Thus, this scheme is not very promising.

CHAPTER 4

Complex Association Schemes

In the previous section, we analyzed the simplistic association scheme where the users either connect with the first nearest or second nearest base station with fixed probabilities. This scheme reduces the rate variance among the users but the average rate of an user decreases significantly. Hence, more complex schemes are simulated where we take more base stations into consideration while finding an associating base station for an user. A SINR biasing scheme is also simulated for a single tier and a 3-tier cellular network.

4.1 Least load allocation

In this scheme, all the nearest neighbors of the base station closest to the user are taken into consideration. The user is linked with a base station in this subset of base stations, which serves the minimum number of users. By associating an user in this manner, more bandwidth will be allocated to the user as there will be less number of users using the same resource. However, the SINR will, fall as the associating base station will be farther. The plots 4.1, 4.2 and 4.3 are obtained from the simulation of this scheme.

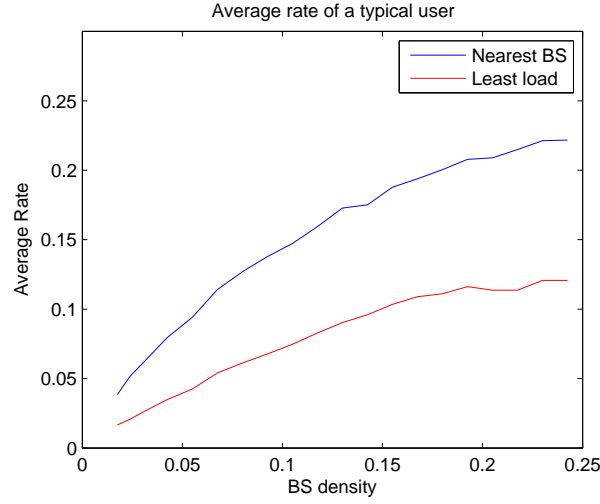


Figure 4.1: The above plot shows the variation of average rate with increasing base station density. The density of users $\lambda_u = 0.8$. It is seen that the rate increases with base station density and converges to a value in both the association schemes.

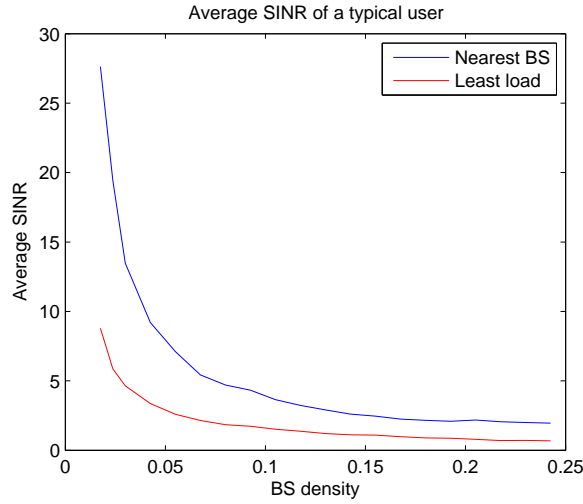


Figure 4.2: The above plot shows the variation of average SINR with increasing base station density. The density of users $\lambda_u = 0.8$. It is seen that the SINR of a typical user sharply decreases and remains constant for high base station densities. Further, it is seen that the nearest BS scheme gives a higher SINR.

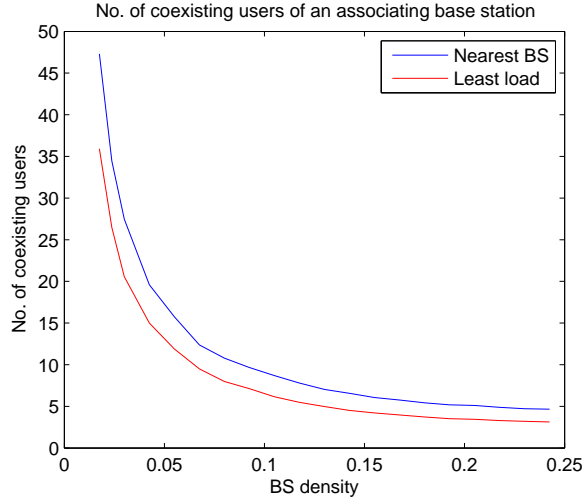


Figure 4.3: The above plot shows the variation of the average number of users of an associating base station with increasing base station density. The density of users $\lambda_u = 0.8$. It is seen that the average number of users of an associating base station is lesser for the bandwidth maximizing scheme.

From figure 4.1, we note that this scheme also does not improve the rate. The decrease in SINR is still not compensated by the increased bandwidth that might be available to the user.

4.2 SINR biasing

In this section, a simple range expansion scheme based on SINR biasing is simulated. In a max-SINR scheme, the user connects with the base station that provides the maximum SINR as the name suggests. Such a scheme will always give a higher SINR than the nearest BS association scheme as the fading loss is also taken into account before choosing a base station. In a SINR bias scheme, a subset of the base stations, say the relatively small base stations, are given a multiplicative bias. If BS 1 had a 10 dB SINR bias

vs. BS 2, a user would associate with it, until the SINR delivered by BS 2 is a full 10 dB higher than that of BS 1. Hence, by giving a higher bias to smaller base stations, the load can be balanced more evenly.

4.2.1 Single-Tier Network

The SINR bias scheme is first implemented in a single-tier network. All base stations which have less than 80% of the average number of users in their coverage area are given a bias. Thus, the range of these small BSs will expand. The results of this simulation is seen in figure 4.4.

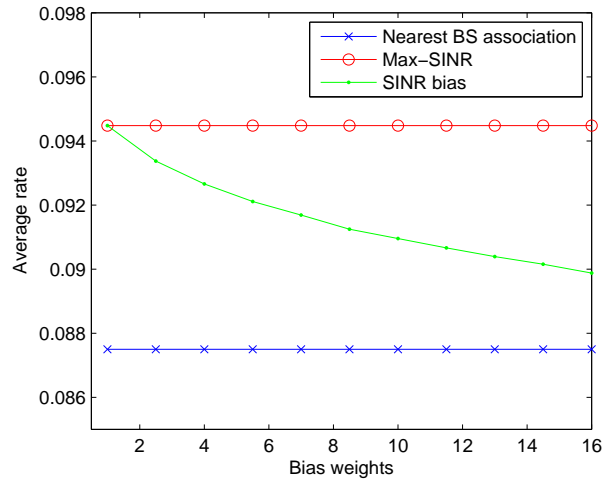


Figure 4.4: The SINR bias scheme is compared with the max-SINR and the nearest BS scheme for a single-tier network. Upon introducing a bias, the average rate of the SINR bias scheme is seen to be lesser than the max-SINR scheme. The increased bandwidth due to load balancing is not enough to improve the rate due to association with BSs providing sub-optimal SINRs.

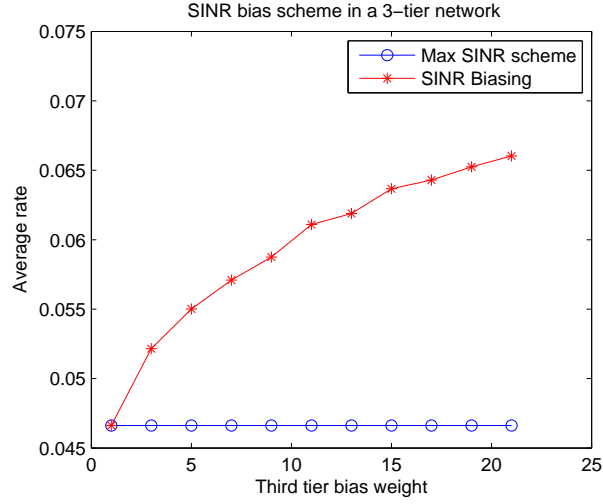


Figure 4.5: The above plot compares the max-SINR scheme with the SINR biasing scheme for a 3-tier cellular network, in terms of mean rate. Bias weights of 1 and 3 are assigned to the first and second tiers. The average rate is then seen to increase with the bias weight of the third tier from the above plot.

4.2.2 Three-tier heterogeneous network

Heterogeneous networks are much more sensitive to cell association policies due to the disparities in cell sizes. Thus, load balancing using SINR bias is performed on a 3-tier cellular network. The three tiers can be viewed as macrocells, picocells and femtocells. The picocells and femtocells which are normally lightly loaded are given a higher bias so that more users connect to these base stations despite sub-optimal SINRs. In the SINR bias scheme simulated, the nearest base station from a user in each tier is found. The user connects to the base station that provides the highest biased SINR out of the 3. In the simulations (Figures 4.6,4.5), the densities of the three tiers are assumed to $\lambda = \{0.01, 0.05, 0.2\}$ and their respective transmit powers are $\{P_1, P_2, P_3\} = \{40, 3, 0.1\}W$.

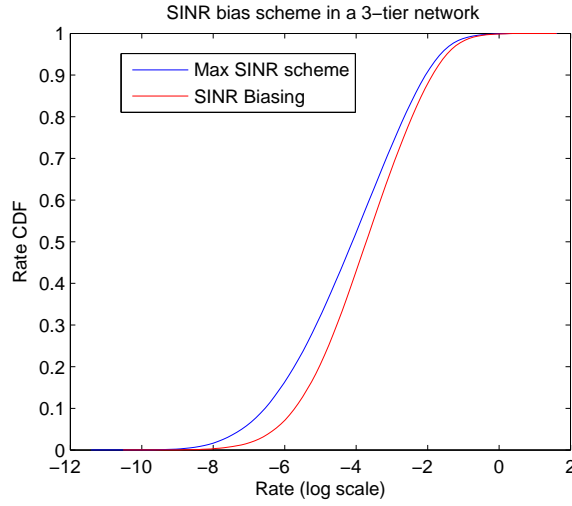


Figure 4.6: For the 3-tier cellular network described in 4.2.2, bias weights of 1, 3 and 20 are assigned to the 1st, 2nd and 3rd tiers respectively. The rate CDF of the SINR biasing scheme is then obtained as above. Note that the rates of edge users are particularly boosted by the SINR bias scheme.

The SINR biasing scheme has been shown to give excellent results in (7) for heterogeneous networks. However, for a single tier network, this scheme does not perform as well (Refer figures 4.4 and 4.5).

CHAPTER 5

Conclusions and future work

In today's cellular networks, the rate distribution and not the SINR is the desired performance metric. The traditional nearest BS association scheme which serves to give a high SINR can be sub-optimal. Hence, another cell association scheme in which the user connects either with the nearest or second nearest base stations with fixed probabilities, is introduced. For single tier networks, this association scheme decreases the mean rate achievable by a typical user. However, the rate variance among users decreases which suggests a more fair treatment of users. Moreover, the load is more evenly balanced among the base stations as a result of this scheme. A SINR biasing scheme was also simulated and compared with the max-SINR and nearest BS association scheme. This SINR biasing scheme does not give a higher mean rate than the max-SINR scheme in a single-tier network. However, this SINR bias scheme is found to give better quality of service in a 3-tier heterogeneous network, in which the BSs in different tiers differ in their density of deployment and power. In (7), the biasing scheme is shown to be nearly as optimum as a centralized rate optimization scheme for heterogeneous networks. A better understanding of the use of biasing schemes in heterogeneous networks, can help optimize the rate distribution of users even further. For single-tier networks, dynamic cell association schemes in which the base stations can change their characteristics depending upon load conditions, can potentially give better results.

REFERENCES

- [1] Andrews JG, Baccelli F, Ganti RK, “A Tractable Approach to Coverage and Rate in Cellular Networks”, IEEE Transactions on Communications, January 2010.
- [2] Andrews JG, “Seven Ways that HetNets Are a Cellular Paradigm Shift”, IEEE Communications Magazine, March 2013.
- [3] Goldsmith A.J. , “Wireless Communications”, Cambridge University Press, 2005.
- [4] Rappaport T.S, “Wireless Communications: Principles and Practice”, 2nd ed. Upper Saddle River, New Jersey: Prentice-Hall, 2002.
- [5] Stoyan D, Kendall W.S and Mecke J, “Stochastic Geometry and its Applications”, John Wiley & Sons, 2008.
- [6] Baccelli F, Blaszczyzyn B, “Stochastic Geometry and Wireless Networks”, NOW: Foundations and Trends in Networking, 2010.
- [7] Q. Ye et al., “User Association for Load Balancing in Heterogeneous Cellular Networks”, IEEE Trans. Wireless., <http://arxiv.org/abs/1205.2833>, to appear.

- [8] Baccelli F., Klein M., Lebourges M., and Zuyev S., "Stochastic geometry and architecture of communication networks", J. Telecomm. Syst., vol. 7, no. 1, pp. 209-227, 1997.
- [9] Baccelli F. and Zuyev S., "Stochastic geometry models of mobile communication networks", Frontiers in Queueing. CRC Press, 1997, pp. 227-243.
- [10] S. Corroy, L. Falconetti, and R. Mathar, "Dynamic cell association for downlink sum rate maximization in multi-cell heterogeneous networks," in IEEE International Conference on Communications (ICC), to be published after Apr. 2012.
- [11] H. Jo, Y. Sang, P. Xia, and J. Andrews, "Heterogeneous cellular networks with flexible cell association: a comprehensive downlink SINR analysis," submitted to IEEE Trans. on Wireless Communications, July 2011, available at arxiv.org/abs/1107.3602.
- [12] Y. Bejerano and S. J. Han, "Cell breathing techniques for load balancing in wireless LANs," IEEE Transactions on Mobile Computing, vol. 8, pp. 735-749, June 2009.